Tanzania Journal of Science 49(3): 605-614, 2023
ISSN 0856-1761, e-ISSN 2507-7961

An Overlapped Sub-array Hybrid Beamforming Architecture with Successive Interference Cancellation and Water-filling in Massive MIMO Systems

Godwin Mruma Gadiel
University of Dar es Salaam, College of Information and Communication Technologies, Department of Electronics and Telecommunications Engineering, P.O. Box 33335, Dar es Salaam, Tanzania. E-mail: gmruma@udsm.ac.tz
ORCID ID: https://orcid.org/0000-0003-0212-1466
Received 14 Apr 2023, Revised 6 Jul 2023, Accepted 16 Aug 2023 Published Sep 2023
DOI: https://dx.doi.org/10.4314/tjs.v49i3.5

Abstract

Over the years, wireless communication has significantly improved the data rate of mobile users. The key drive behind this success is the technological advancement in wireless communication. In the physical layer, hybrid beamforming has revolutionized the way signal reaches the user by constructively adding the signal at the destination thus improving the performance. Many researchers works have proposed different algorithms to solve for optimal hybrid beamforming. However, there is no single algorithm that can achieve both high spectral efficiency and energy efficiency at the same time. This work proposes a hybrid algorithm that combines successive interference cancellation and water filling and applies this algorithm in overlapped sub-array architecture (OSA). The former can successfully optimize for analog precoding in a subarray environment as it eliminates the interference between the successive sub-arrays. While the latter can allocate the power in each data stream proportionally, thus improving the spectral efficiency. The simulation results show that the proposed algorithm with OSA can achieve a near optimal performance in comparison to fully connected hybrid beamforming (FCH) and significantly larger performance in comparison to partially connected hybrid beamforming (PCH). Moreover, the proposed algorithm achieves 89.2% energy efficiency in comparison to PCH architecture. These results show that an OSA system with the proposed algorithm provides a better tradeoff between achieved spectral efficiency (SE) and energy efficiency (EE).

Keywords: mmWave, massive MIMO, Hybrid beamforming, Energy efficiency, 5G.

Introduction

A multi gigabit data rate achieved by 5G is enhanced by its physical layer which employs a massive MIMO system (Akpakwu et al. 2017, Li et al. 2019, Xue et al. 2020). Massive MIMO technology employs a large number of antennas at the base station (BS) (Han et al. 2015). By doing so, the base station can direct power toward the intended users through beamforming techniques. Initially, beamforming was achieved through digital beamforming architecture, where each antenna is connected to a dedicated radio frequency (RF) chain (Kim et al. 2011). These RF chains are comprised of power hungry devices, such as digital to analog converter on the transmitter side and analog to digital converter on the receiver side (Ayach et al. 2012, Gao et al. 2016, Mendez-Rial et al. 2016, Nguyen et al. 2017). For the case of massive MIMO, a large number of antennas will lead to a large number of RF

chains, which will significantly increase the power consumption of a transceiver. In addition, the large dimension of the matrix in the massive MIMO, adds computational complexity constraints in digital beamforming processing.

To address these challenges, an analog based beamforming architecture that employs phase shifters before each antenna was poposed (Nsenga et al. 2009). However, its performance was low compared to digital beamforming. To improve the performance and yet provide a reasonable power consumption, a hybrid beamforming architecture was proposed by researchers (Ayach et al. 2014, Liang et al. 2014, Mendez-Rial et al. 2016). Hybrid beamforming architecture is comprised of analog beamforming, where a single RF chain is connected to multiple antenna and RF chains are connected to a digital processor for digital beamforming. This configuration reduces the number of RF chains, and the matrix dimension is also significantly lowered (Mendez-Rial et al. 2016).

There are three types of hybrid beamforming architecture: Fully connected hybrid beamforming (FC-HBF) architecture, overlapped sub-array architecture (OSA), and partially connected hybrid beamforming (PC-HBF) architecture (Akpakwu et al. 2017, Song et al. 2017, Sourour 2019). In the first one, each RF chain is connected to all antennas, the second one each RF chain is connected to a specific number of antennas but few antennas are overlapped, whereas, the last one, each RF chain is connected to specific number of antennas without overlapping. The FC-HBF can achieve high performance near digital beamforming architecture (Sohrabi and Yu 2016, Yu et al. 2016). However, when the number of phase shifter is large, its power consumption becomes large compared to digital beamforming (Xu et al. 2017, Xue et al. 2020).

The PC-HBF can significantly improve power consumption as the number of phase shifter are limited to N_t, however, its spectral efficiency performance is low compared to FC-HBF (Sohrabi and Yu 2016,Yu et al. 2016). Several initiatives have been done to improve the performance of PC-HBF, by proposing algorithms which will significantly improve the performance (Gao et al. 2016, Park et al. 2017, Li et al. 2017, Li et al. 2019, Nguyen and Lee 2020, Gadiel et al. 2021). One of the approaches used successive interference cancellation in the analog beamforming and in the digital beamforming a block diagonal power allocation was used (Gao et al. 2016). However, the spectral efficiency did not improve near to the FC-HBF.

In this work, the researcher proposes to use OSA by taking advantage of overlapped sub-array to improve performance. In addition, the researcher proposes to apply the interference cancellation method in the analog beamforming and further improve the performance of the system by using a water-filling algorithm in the digital beamforming. The power allocation in each data stream depends on the effective channel of the particular data stream. The simulation results show that the proposed architecture and the algorithm can significantly improve performance. Additionally, the power consumption is significantly lowered by limiting the number of overlapped phase shifters to the near optimal value while achieving high spectral efficiency. With the simulation results, it is evident that when the spectral efficiency of OSA is optimized, the tradeoff between the achieved spectral efficiency and energy efficiency can be achieved.

Materials and Methods

In this work, a mathematical model of the system under study has been presented. Furthermore, a computer simulation is used to analyze the system performance of the proposed architecture. This section presents the system model and the proposed algorithm. Additionally, the computational complexity of the proposed algorithm and the energy efficiency of the proposed architecture are discussed.

A. System model

In this section, the system model for point to point massive MIMO system using OSA is presented and the problem is formulated.

A single-user mmWave system shown in Figure 1 is considered, i.e., the overlapped sub-array architecture. In this setting, N_t transmit antennas communicates N_s data stream to a receiver with N_r antennas, and $\triangle N$ is the number of overlapped antennas (Song et al. 2017). The transmitter is equipped with N_{RF} RF chains, which enables muti-stream data communication between transmitter and receiver, where $N_s \leq N_{RF} \leq N_t$. The transmitted signal from this setting is denoted as $\boldsymbol{x} = \boldsymbol{F}_{RF}\boldsymbol{F}_{BB}\mathbf{s}$, where the transmitted symbol vector $\boldsymbol{s} \in \mathbb{C}^{N_s \times 1}$ is first precoded by digital baseband precoder $\boldsymbol{F}_{BB} \in \mathbb{C}^{N_{RF} \times N_s}$ and then followed by analog RF precoder $\boldsymbol{F}_{RF} \in \mathbb{C}^{N_t \times N_{RF}}$. The transmitted symbol vector s is such that $\mathbb{E}[\boldsymbol{s}\boldsymbol{s}^*] = \frac{1}{N_s}\mathrm{I}_{N_s}$. Whereas, the transmit hybrid precoder is assumed to have normalized transmit power constraint such that, $\| \boldsymbol{F}_{RF}\boldsymbol{F}_{BB} \|_F^2 = N_s$. To fully exploit the spatial multiplexing gain, this work assumes $N_s = N_{RF}$ (Han et al. 2015). Therefore, the received signal is given by

$$\boldsymbol{y} = \sqrt{\rho}\boldsymbol{H}\boldsymbol{x} + \boldsymbol{n}, \qquad (1)$$

where $\boldsymbol{y}$ is the $N_r \times 1$ received vector, $\boldsymbol{H}$ is the $N_r \times N_t$ channel matrix such that $\mathbb{E}[\| \boldsymbol{H} \|_F^2] = N_t N_r$, ρ presents the average received power and n is an additive white Gaussian noise (AWGN) vector, whose entries follow the independent and identical distribution (i.i.d) $\mathcal{CN}(0, \sigma^2)$.

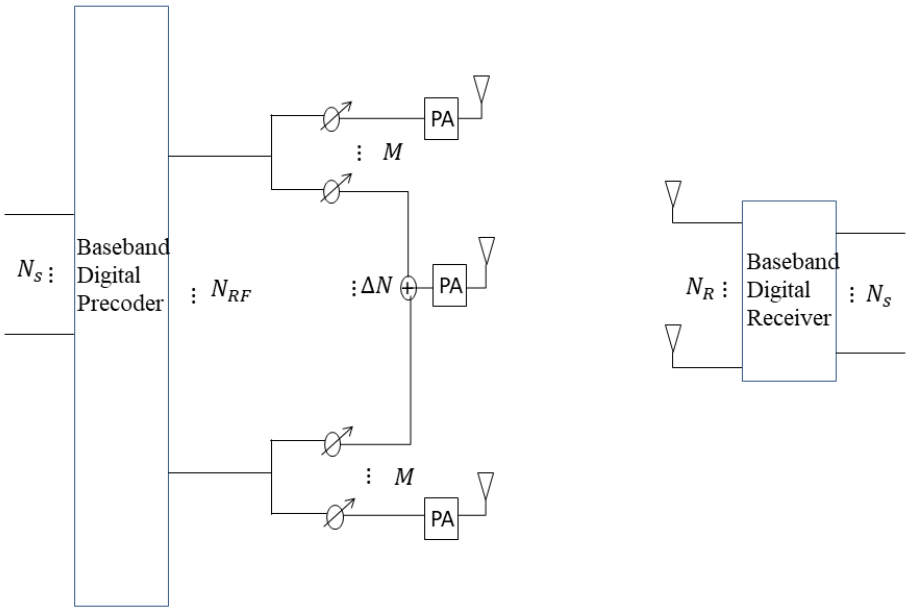

Figure 1: OSA based mmWave single user system.

Because the architecture is an overlapped sub-array, the analog precoding matrix is given by

$$\boldsymbol{F}_{RF} = \begin{Bmatrix} \boldsymbol{f}_1(1) & 0 & \cdots & 0 \\ \vdots & f_2(1) & \cdots & 0 \\ \boldsymbol{f}_1(M) & \vdots & \cdots & \vdots \\ 0 & \boldsymbol{f}_2(M) & \ddots & \boldsymbol{f}_{N_{RF}}(1) \\ 0 & 0 & \cdots & \vdots \\ 0 & 0 & \cdots & \boldsymbol{f}_{N_{RF}}(M) \end{Bmatrix} \quad (2)$$

where M is the number of elements in a given sub-array and $\boldsymbol{f}_{i,j} = \frac{1}{M} e^{j\theta_{i,j}}$, whereas, $\theta_{i,j}$ is the phase value of (i,j)th phase shifter. This paper focuses on optimizing hybrid precoding at the transmitter, and assumes perfect decoding at the receiver. Thus, the total data rate achieved by Gaussian signalling simplifies to the channel's mutual information which can be given as

$$R = log_2 \left| I_{N_r} + \frac{\rho}{N_s \sigma} \boldsymbol{H}\boldsymbol{F}\boldsymbol{F}^H \boldsymbol{H}^H \right|, \quad (3)$$

where $\boldsymbol{F} = \boldsymbol{F}_{RF} F_{BB}$ is the overall precoding matrix at the transmitter. The aim is to find the optimal $\boldsymbol{F}$ such that the total achievable rate in Equation (3) is maximized.

B. Proposed Algorithm

In this work, the optimal precoder matrix $\boldsymbol{F}$ is obtained in two stages. Where, in the first stage a digital precoder is assumed to be $\boldsymbol{F}_{BB} = \boldsymbol{I}_{N_s}$, therefore we use successive interference cancellation to obtain the analog precoding F_{RF}. Thus, solving for analog precoder, Equation (3) can be modified to

$$R_1 = \log_2 \left| \mathrm{I}_{N_r} + \frac{\rho}{N_s \sigma} \mathbf{H}\mathbf{F}_{RF}\mathbf{F}_{RF}^H \mathbf{H}^H \right| \quad (4)$$

To solve R_1, first the analog precoder matrix is decomposed into $\boldsymbol{F} = \left[\boldsymbol{F}_{RF}^{N_{RF}-1} \boldsymbol{f}^{N_{RF}}\right]$, where $\boldsymbol{f}^{N_{RF}}$ is the N_{RF}th column of $\boldsymbol{F}_{RF}$. Then, the total achievable data rate Equation 4, can be decomposed into N_{RF} sub total rate, and the total sum rate can be given by

$$R_1 = \sum_{n=1}^{N_{RF}} \log_2 \left| 1 + \frac{\rho}{N_s \sigma^2} \boldsymbol{f}_n^H \boldsymbol{H}^H \boldsymbol{T}_{n-1}^{-1} \boldsymbol{H}\boldsymbol{f}_n \right| \quad (5)$$

where $\boldsymbol{T}_n = \boldsymbol{I}_{N_r} + \frac{\rho}{N_s \sigma^2} \boldsymbol{H}\boldsymbol{F}_{RF}^n (\boldsymbol{F}_{RF}^n)^H \boldsymbol{H}^H$ and $\boldsymbol{T}_0 = \boldsymbol{I}_{N_r}$. To find the optimal RF precoder that solve Equation (5), we utilize the successive interference algorithm as used in Gao et al. (2016). The modified version only search for $\theta_{i,j} = \angle(\boldsymbol{v}_{i,1})$, where $\boldsymbol{v}_1$ is the optimal unconstrained precoder vector.

After obtaining the optimal analog precoder in the first stage, the second stage optimizes the total achievable rate by finding the optimal digital precoder. When we have the analog precoder matrix, the effective channel can be defined as $\boldsymbol{H}_e = \boldsymbol{H}\boldsymbol{F}_{RF}$. Therefore, the total achievable rate in Equation 3 can be modified to

$$R_2 = \log_2 \left(\left| \mathrm{I}_{N_r} + \frac{\rho}{N_s \sigma^2} \boldsymbol{H}_e \boldsymbol{F}_{BB} \boldsymbol{F}_{BB}^H \boldsymbol{H}_e^H \right| \right) \quad (6)$$

The optimal solution of $\boldsymbol{F}_{BB}$ in Equation (6), can be found by water-filling algorithm and it is given by

$$\boldsymbol{F}_{BB} = \boldsymbol{Q}_e^{-1/2} \boldsymbol{U}_e \boldsymbol{L}_e, \quad (7)$$

where $\boldsymbol{U}_e$ is the right singular vectors corresponding to N_s largest singular values of $\boldsymbol{H}_{eq}\boldsymbol{Q}_e^{-1/2}$ and L_e is the diagonal matrix of allocated power in each stream. According to Sohrabi and Yu (2016) , $\boldsymbol{F}_{BB}\boldsymbol{F}_{BB}^H \propto \boldsymbol{I}$, and this is true if and only if N_t is approximately large as for the case of massive MIMO. Assuming equal power allocation in each data stream $\boldsymbol{L}_e \approx \sqrt{\rho/N_s}\boldsymbol{I}$, and therefore the near optimal digital precoder can be approximated as $\boldsymbol{F}_{BB} \approx \gamma \boldsymbol{I}$, where $\gamma^2 = \rho/N_s$. To further improve this solution, this work proposes unequal power allocation based on the singular values of $\boldsymbol{H}_e$. The proposed algorithm is summarized in Table 1.

Table 1: Proposed algorithm

Required: $\boldsymbol{H}, \mathcal{F}$,
Output: $\boldsymbol{F}_{RF}, \boldsymbol{F}_{BB}$,

1. Apply SIC to obtain F_{RF} as in Gao et al. (2016)
2. Compute $[\boldsymbol{U}, \boldsymbol{S}, \boldsymbol{V}]$ =svd$(\boldsymbol{H}_e)$,
3. Compute water levels $\gamma_1, \gamma_2, \ldots, \gamma_{N_s}$ based on $\boldsymbol{S}$,
4. $\boldsymbol{F}_{BB} = diag\{\gamma_1, \gamma_2, \ldots, \gamma_{N_s}\}$

C. Computational complexity analysis

In this subsection, computational complexity analysis of the proposed algorithm is performed. Computational complexity is defined as the number of complex multiplications. In the proposed algorithm, the complexity comes from serial 1 of the algorithm where successive interference cancelation algorithm is used to obtain the analog precoder. The number of complex multiplication is $N^2(N_{RF}W + N_r)$, where W is the number of maximum iterations in the SIC algorithm (Gao et al. 2016). Serial 2, also contributes to the complexity of the proposed algorithm, where a digital precoder is obtained. Specifically, the complexity comes from the SVD decomposition of the equivalent channel in line 2, where there are $21N_r^3$ complex multiplications. Therefore, the total computational complexity for the proposed algorithm is $N^2(N_{RF}W + N_r) + 21N_r^3$. Complexity comparison for different algorithms is described in Table 2. From Table 2, the computational complexity of the proposed algorithm is slightly large compared to SIC based algorithm, however, the performance of the proposed algorithm is larger compared to other algorithms as will be seen in the results and discussion sections.

Table 2: Complexity comparison for different algorithms

	Number of complex multiplications
SIC based algorithm (Gao et al. 2016)	$N^2(N_{RF}W + N_r)$
Spatially sparse precoding (Ayach et al. 2014)	$N_{RF}^4M + N_{RF}^2L^2 + N_{RF}^2M^2L$
Proposed Algorithm	$N^2(N_{RF}W + N_r) + 21N_r^3$

D. Energy efficiency analysis

In this subsection, the paper discusses the energy efficiency of overlapped sub-array hybrid beamforming architecture in comparison with other architectures. Energy efficiency is defined as the ratio between the achieved spectral efficiency over the circuit's total power consumption (Mendez-Rial et al. 2016). The total power consumption of OSA architecture is given by

$$P_{Cons} = MN_{RF}^tP_{PS} + N_{RF}^t(P_{RF} + P_{DAC}) + P_{BB}, \tag{8}$$

where P_{PS}, P_{RF}, P_{DAC} and P_{BB} are power consumption of the phase shifters, RF chain, DAC and base band processor, respectively. The results and discussion section presents the energy efficiency of OSA and other architectures. The power consumption value for each component used in the simulation is defined in Mendez-Rial et al. (2016).

Results and Discussions

This section discusses the simulation results of the proposed algorithm in the mmWave channel environment. This work adopts Saleh-Valenzuela channel model to embody the low rank and spatial correlation characteristics of mmWave communications (Ayach et al. 2014, Mendez-Rial et al. 2016, Gao et al. 2016, Sohrabi and Yu 2016) as

$$\boldsymbol{H} = \sqrt{\frac{N_tN_r}{L_p}}\sum_{l=1}^{L_p}\alpha_l\,\Lambda_r(\phi_l^r,\theta_l^r)\Lambda_t(\phi_l^t,\theta_l^t)\boldsymbol{f}_r(\phi_l^r,\theta_l^r)\boldsymbol{f}_t^H(\phi_l^t,\theta_l^t) \tag{9}$$

where L_p is the number of effective channel paths corresponding to the limited number of scatters. α_l is the complex gain of the l^{th} ray, whereas $\phi_l^r,(\theta_l^r)$ and $\phi_l^t,(\theta_l^t)$ are its azimuth (elevation) angles of arrival and departure, respectively. The transmit and receive antenna element gain at the corresponding angles of departure and arrival, are calculated by the functions $\Lambda_t(\phi_l^t,\theta_l^t)$ and $\Lambda_r(\phi_l^r,\theta_l^r)$, respectively. Finally, $\boldsymbol{f}_r(\phi_l^r,\theta_l^r)$ and $\boldsymbol{f}_t^H(\phi_l^t,\theta_l^t)$ are the antenna array response vectors depending on the antenna array structure at the base station and user,

respectively. This work adopts uniform linear array (ULA), with U elements in transmitter and receiver, and the response vector can be given by (Ayach et al. 2014)

$$\boldsymbol{f}_{ULA}(\phi) = \frac{1}{\sqrt{U}}\left[1, e^{j\frac{2\pi}{\lambda}dsin(\phi)}, \ldots, e^{j(U-1)\frac{2\pi}{\lambda}dsin(\phi)}\right]^T \quad (10)$$

where λ denotes the wavelength of the signal, and d is the antenna spacing. The subscripts (r, t) in Equation (9) are abondoned and the elevation angle θ is not included, because, the ULA response vector is independent of elevation angle.

The simulation results presented in this work consider the environment where $L_p = 10$ scatterers between transmitter and receiver are available. Also, uniform random angles of arrival and departure are considered. The spacing between antennas is considered to be $d = \frac{\lambda}{2}$, and signal to noise ratio is defined as $\frac{P}{\sigma^2}$ over 2000 channel realization.

First, the paper evaluates the achievable spectral efficiency versus different SNR values, where perfect channel state information (CSI) is assumed, and the corresponding simulation results are presented in Figure 2. The SIC algorithm is applied to the overlapped sub-array architecture, where it shows an inferior performance in comparison to our proposed algorithm, which is a hybrid of SIC and water filling algorithms. It can be seen from the simulation results, OSA architecture can achieve appreciable spectral efficiency in comparison to partially connected architecture just by adding few antennas in a sub-array through overlapping phenomenon. Specifically, in this simulation results, each RF chain in OSA was connected to 28 phase shifters compared to 16 phase shifters in each RF chain of PCH. With this configuration, at $SNR = 10\ dB$, the proposed algorithm can achieve 93.1% of the fully connected architecture, while SIC algorithm on PCH can achieve 81.6%.

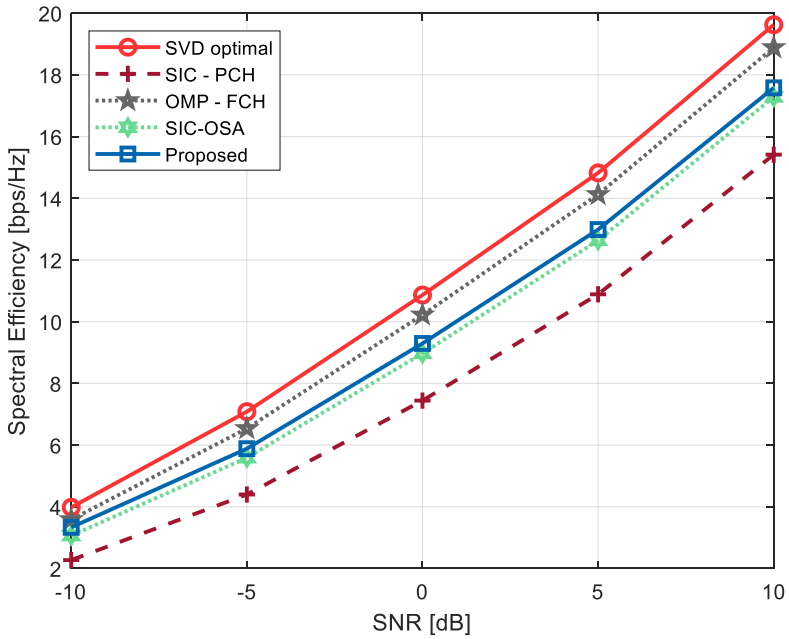

Figure 2: Spectral efficiency comparison for different SNR values for a massive MIMO system with $N_t = 64$, $N_{RF}^t = 4$ and $N_r = 16$.

Figure 3 demostrates the spectral efficiency in comparison to different number of antennas, whereas for each BS antenna set, the number of phase shifters in each RF chain for OSA system was {28,53,130,239}, respectively. The proposed algorithms outperforms the conventional SIC algorithm, when they are both applied in OSA architecture. It is observed that, as the number of antennas increases, the spectral efficiency also increases. Particularly, when $N_t = 512$, the proposed algorithm achieves 92.9% of the fully connected hybrid beamforming architecture, while partially connected hybrid beamforming architecture achievs 78.3% in comparison to FCH.

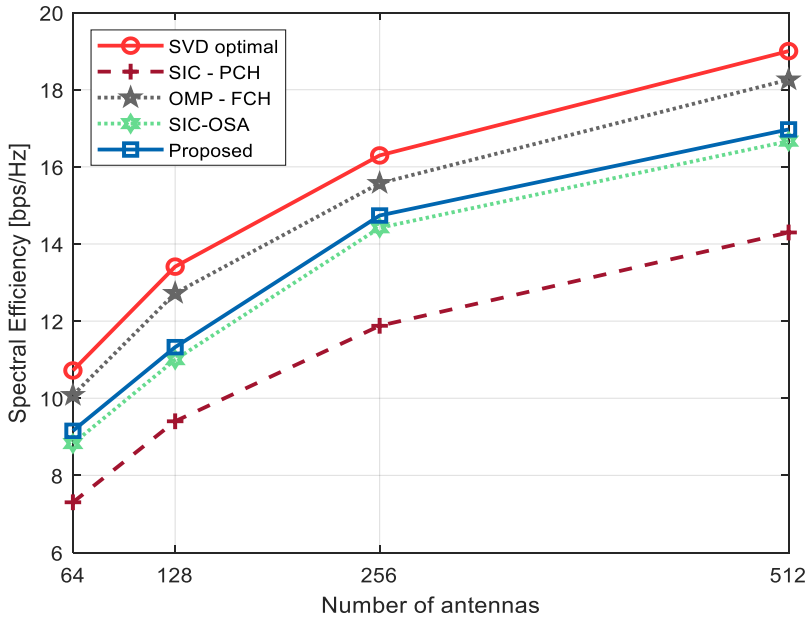

Figure 3: Spectral efficiency comparison aganinst the number of BS antennas, where $N_r = 16$, $N_{RF}^t = 4$ and $SNR = 0\ dB$.

Figure 4 shows the achievable spectral efficiency in comparison to the number of receiver antennas when SNR = 0 dB. It is observed that, for both algorithms, the spectral efficiency is lower when the number of receive antenna is small. The performance increases, as the number of receive antennas increases and it reach a point where the performance increase is not significant. Furthermore, the proposed algorithm when applied to OSA, it achieves 88.2% of the FCH architecture, while SIC on PCH architecture can only achieve 73% , when the number of antennas at the receiver is 32.

Moreover, the paper evaluates the achieved spectral efficiency in relation to the number of RF chains for different number of antennas and the results are shown in Figure 5. It is observed that, when the number of RF chains increases, the achieved spectral efficiency also increases. The proposed algorithm as applied in OSA can achieve appreciable results in comparison with fully connected hybrid beamforming architecture. Particularly, when there are 8 RF chains, the number of antennas (N_t) are 512 and the number of elements (M) in each RF chain of OSA architecture are 141, the proposed algorithm achieves 96.3% that of fully connected architecture. It is also observed that, the PCH with SIC algorithm achieves 78.4% in comparison to fully connected architecture. The results showed that, we can utilize OSA architecture and achieve a performance near to FCH architecture.

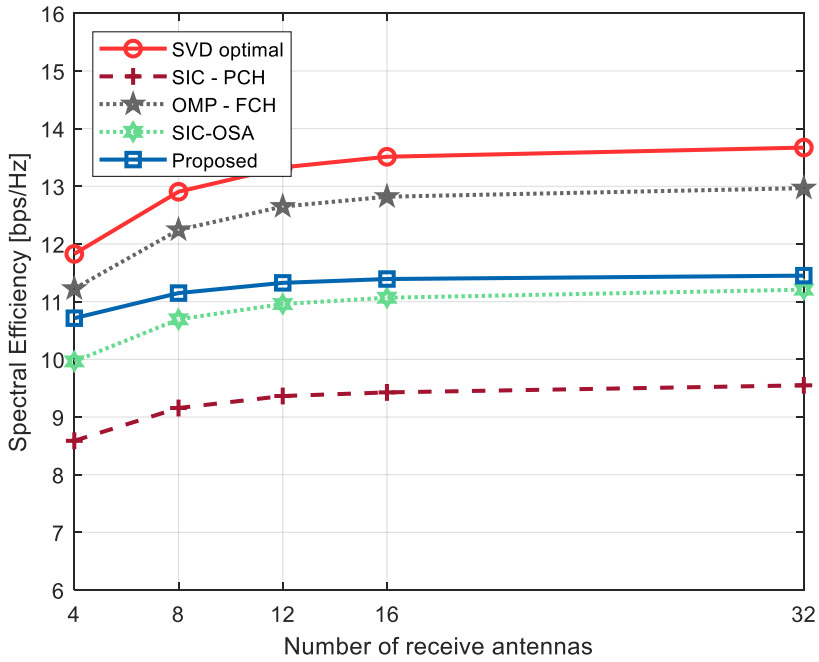

Figure 4: Spectral efficiency comparison aganinst the number of receiver antennas, where $N_t = 128$, $N_{RF}^t = 4$ and $SNR = 0\ dB$.

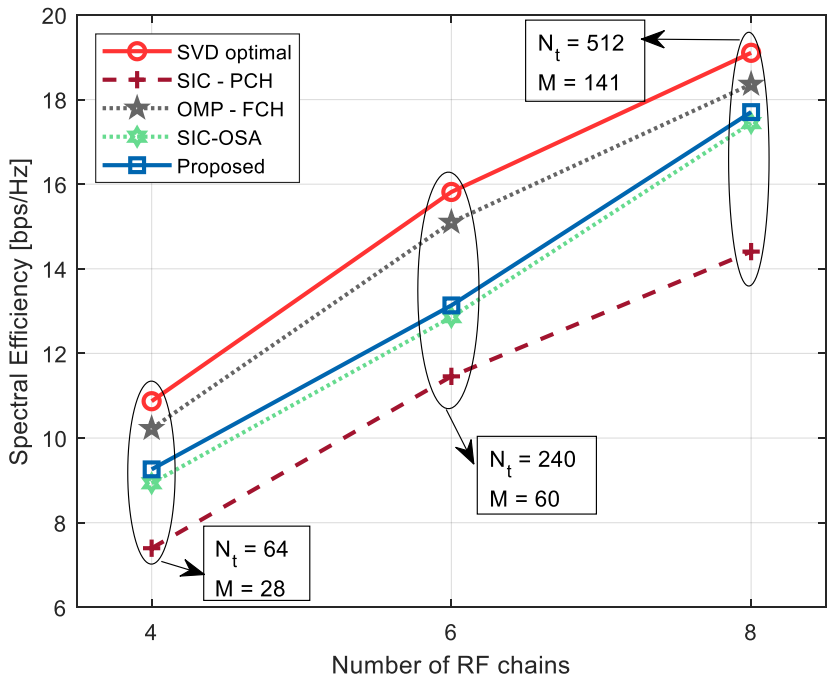

Figure 5: Achieved spectral efficiency comparison against different number of RF chains, where $SNR = 0\ dB$.

Finally, the paper analyzes the energy efficiency performance for the proposed algorithm as applied to OSA in comparison to FCH and PCH architectures as shown in Figure 6. It is observed that, the proposed algorithm achieves a close performance in comparison to PCH architecture. The energy efficiency of the proposed algorithm in comparison with FCH architecture is significantly large. Specifically, when the number of antennas are 512 and the number of antennas connected in each RF chain in OSA are 239, the energy efficiency gap between the proposed algorithm and FCH is 44.5%. Whereas, the energy efficiency gap between PCH and proposed algorithm is only 12.1%. The results showed that, OSA can achieve a better tradeoff between the achieved spectral efficiency and energy efficiency, when an appropriate algorithm is applied on OSA.

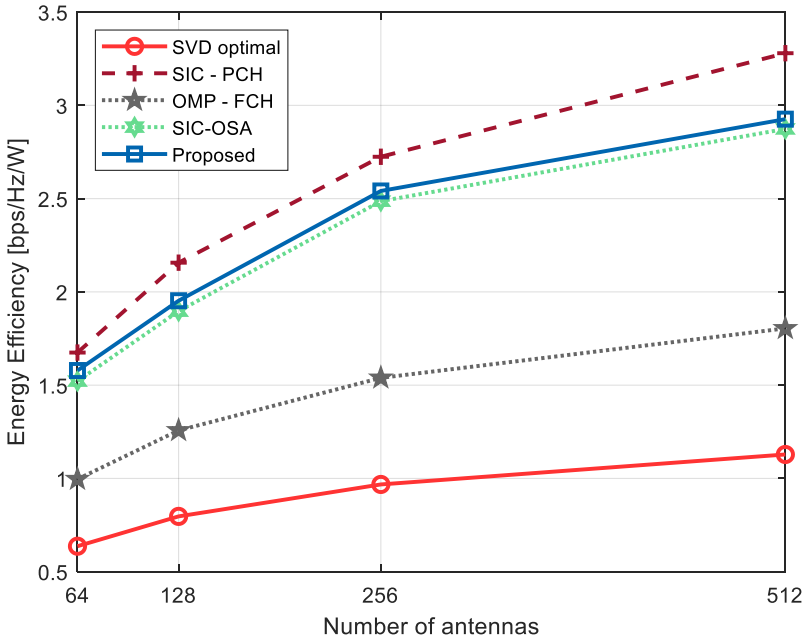

Figure 6: Energy efficiency versus number of antennas, where $SNR = 0\ dB$.

Conclusions

This paper proposes a SIC algorithm for analog precoding and a water filling algorithm for digital precoding in an OSA based massive MIMO system. First, the paper showed that the SIC can be applied in OSA to solve for analog precoding assuming that each sub-array is an independent entity. Additionally, having analog precoding, it has been shown that the near optimal digital precoding can be found by applying a water filling algorithm. The combination of the two algorithms has shown superiority in solving for analog and digital precoding in OSA. Even though the computational complexity slightly increased, the achieved spectral efficiency is significant. Simulation results show that the proposed algorithm achieves a better performance in comparison to the conventional SIC algorithm. Specifically, the proposed algorithm achieves 93.1% at an SNR = 10 dB in comparison to OMP-FCH. Furthermore, the proposed algorithm achieves 89.2% of energy efficiency in comparison to conventional SIC under PCH architecture. In the future, this work will be extended to study the performance of the proposed algorithm under imperfect CSI.

References

Akpakwu GA, Silva BJ, Hancke GP and Abu-Mahfouz AM 2017 A survey on 5G

networks for the Internet of Things: Communication technologies and challenges. *IEEE Access* 6: 3619–3647.

Ayach O El, Heath RW, Abu-Surra S, Rajagopal S and Pi Z 2012 Low complexity precoding for large millimeter wave MIMO systems. *IEEE Int. Conf. Commun.* 3724–3729.

Ayach O El, Rajagopal S, Abu-Surra S, Pi Z and Heath RW 2014 Spatially sparse precoding in millimeter wave MIMO systems. *IEEE Trans. Wireless Commun.* 13(3): 1499–1513.

Gadiel GM, Nguyen NT and Lee K 2021 Dynamic unequally sub-connected hybrid beamforming architecture for massive MIMO systems. *IEEE Trans. Veh. Technol*. 70(4): 3469–3478.

Gao X, Dai L, Han S, Chih-Lin I and Heath RW 2016 Energy-efficient hybrid analog and digital precoding for MmWave MIMO systems with large antenna arrays. *IEEE J. Select. Areas Commun.* 34(4): 998–1009.

Han S, I C, Xu Z and Rowell C 2015 Large-scale antenna systems with hybrid analog and digital beamforming for millimeter wave 5G. *IEEE Commun. Mag*. 53(1): 186–194.

Kim K, Ko K and Lee J 2011 Adaptive selection of antenna grouping and beamforming for MIMO systems. *Eurasip J. Wireless Commun. Network* 2011: 2–9.

Li H, Li M and Liu Q 2019 Hybrid beamforming with dynamic subarrays and low-resolution PSs for mmWave MU-MISO systems (61671101).

Li N, Wei Z, Yang H, Zhang X and Yang D 2017 Hybrid precoding for mmWave massive MIMO systems with partially connected structure. *IEEE Access* 5: 15142–15151.

Liang L, Xu W and Dong X 2014 Low-complexity hybrid precoding in massive multiuser MIMO systems. *IEEE Wireless Commun. Lett*. 3(6): 653–656.

Mendez-Rial R, Rusu C, Gonzalez-Prelcic N, Alkhateeb A, and Heath RW 2016 Hybrid MIMO Architectures for millimeter wave communications: Phase shifters or switches? *IEEE Access* 4: 247–267.

Nguyen DHN, Le LB, Le-Ngoc T and Heath RW 2017 Hybrid MMSE precoding and combining designs for mmWave multiuser systems. *IEEE Access* 5: 19167–19181.

Nguyen NT and Lee K 2020 Unequally sub-connected architecture for hybrid beamforming in massive MIMO systems. *IEEE Trans. Wireless Commun*. 19: 1–11.

Nsenga J, Van Thillo W, Horlin F, Ramon V, Bourdoux A and Lauwereins R 2009 Joint transmit and receive analog beamforming in 60 GHz MIMO multipath channels. *IEEE Int. Conf. Commun*. 25–29.

Park S, Alkhateeb A and Heath RW 2017 Dynamic subarrays for hybrid precoding in wideband mmWave MIMO systems. *IEEE Trans. Wirel. Commun.* 16(5): 2907–2920.

Sohrabi F and Yu W 2016 Hybrid digital and analog beamforming design for large-scale antenna arrays. *IEEE J. Select. Topics Signal Process*. 10(3): 501–513.

Song N, Yang T, and Sun H 2017 Overlapped subarray based hybrid beamforming for millimeter wave multiuser massive MIMO. *IEEE Signal Process. Lett.* 24(5): 550–554.

Sourour E 2019 Codebook-based precoding for generalized spatial modulation with diversity. *Eurasip J. Wireless Commun. Networking* 2019(1).

Xu W, Liu J, Jin S and Dong X 2017 Spectral and energy efficiency of multi-pair massive MIMO relay network with hybrid processing. *IEEE Trans. Commun.* 65(9): 3794–3809.

Xue X, Wang Y, Yang L, Shi J and Li Z 2020 Energy-efficient hybrid precoding for massive MIMO mmWave systems with a fully-adaptive-connected structure. *IEEE Trans. Commun*. 68(6): 3521–3535.

Yu X, Shen JC, Zhang J and Letaief KB 2016 Alternating minimization algorithms for hybrid precoding in millimeter wave MIMO systems. *IEEE J. Select. Topics Signal Process.* 10(3): 485–500.